Published in final edited form as:
Biochem Biophys Res Commun. 2011 May 13; 408(3): 388–392. doi:10.1016/j.bbrc.2011.04.023.

Functional and Physical Competition between Phospholamban and its Mutants Provides Insight into the Molecular Mechanism of Gene Therapy for Heart Failure

Elizabeth L. Lockamy, **Razvan L. Cornea**, **Christine B. Karim**, and **David D. Thomas***
Department of Biochemistry, Molecular Biology and Biophysics, University of Minnesota Medical School, Minneapolis, Minnesota 55455

Abstract

We have used functional co-reconstitution of purified sarcoplasmic reticulum (SR) Ca^{2+}-ATPase (SERCA) with phospholamban (PLB), its inhibitor in the heart, to test the hypothesis that loss-of-function (LOF) PLB mutants (PLB_M) can compete with wild-type PLB (PLB_W) to relieve SERCA inhibition. Co-reconstitution at varying PLB/SERCA ratios was conducted using synthetic PLB_W, gain-of-function mutant I40A, or loss-of-function (LOF) mutants S16E (phosphorylation mimic) or L31A. Inhibitory potency was defined as the fractional increase in K_{Ca}, measured from the Ca^{2+}-dependence of ATPase activity. At saturating levels of these PLB variants, the inhibitory potency of I40A was about three times that of PLB_W, while the potency of each of the LOF PLB_M was about one third that of PLB_W. However, there was no significant variation in the apparent SERCA affinity for these four PLB variants. When SERCA was co-reconstituted with mixtures of PLB_W and LOF PLB_M, inhibitory potency was reduced relative to that of PLB_W alone. Furthermore, FRET between donor-labeled SERCA and acceptor-labeled PLB_W was decreased by both (unlabeled) LOF PLB_M. These results show that LOF PLB_M can compete both physically and functionally with PLB_W, provide a rational explanation for the success of S16E-based gene therapy in animal models of heart failure, and establish a powerful platform for designing and testing more effective PLB_M targeted for gene therapy of heart failure in humans.

Keywords

Ca^{2+}-ATPase; SERCA; fluorescence resonance energy transfer; FRET

1. Introduction

Muscle relaxation occurs when the sarcoplasmic reticulum (SR) Ca^{2+}-ATPase (SERCA) hydrolyzes ATP and pumps Ca^{2+} from the sarcoplasm back into the SR against its concentration gradient. In the heart, SERCA activity is regulated by phospholamban (PLB), a single-span membrane protein that functions to inhibit SERCA by decreasing its apparent Ca-affinity (increasing K_{Ca}) [1]. PLB inhibition of SERCA is relieved physiologically either by micromolar Ca^{2+} or by phosphorylation of PLB at Ser 16 by PKA [2–4], and can also be relieved by a number of point mutations [5], including S16E (a cytoplasmic domain

*To whom correspondence should be addressed: ddt@umn.edu.

mutation that partially mimics phosphorylation [6]) and L31A (a transmembrane domain mutation [5]).

Insufficient SERCA activity is a hallmark of heart failure (HF), which is a leading cause of hospitalization and death in most parts of the world [7], and overexpression of SERCA, using recombinant AAV vectors, has been shown to relieve heart failure in clinical trials [8]. HF is associated with an increased ratio of PLB to SERCA [9], so the inhibitory interaction between SERCA and PLB has become an attractive therapeutic target [2]. Indeed, interfering with the SERCA-PLB interaction in HF animal models can result in improved cardiac function [10–14]. However, complete ablation of PLB can lead to premature death in humans [15], suggesting that a more subtle approach is needed.

Relief of PLB-dependent SERCA inhibition, whether by micromolar Ca^{2+}, PLB phosphorylation, or functional mutation in PLB, has long been thought to require dissociation of the PLB-SERCA complex (Fig. 1A), a hypothesis supported primarily by cross-linking studies [16, 17]. However, this hypothesis is inconsistent with measurements of fluorescence resonance energy transfer (FRET) from SERCA to PLB that demonstrated no Ca^{2+}-dependence of SERCA-PLB affinity [18] and with intra-PLB FRET and electron paramagnetic resonance (EPR) studies that showed no SERCA-PLB dissociation by either Ca^{2+} or phosphorylation of PLB at S16 [19, 20], suggesting that PLB remains bound upon SERCA activation (Fig. 1B). In addition, several loss-of-function (LOF, with less inhibitory potency than WT) PLB mutants have been shown to retain at least some SERCA binding affinity [6, 21, 22]. These results suggest that it might be feasible to identify a LOF PLB mutant (denoted PLB_M below) with sufficient SERCA affinity to compete with WT (denoted PLB_W below) for SERCA binding, and that such a mutant would be a useful therapeutic reagent. Intriguingly, *in vivo* cardiac rAAV delivery of a gene corresponding to S16E, a pseudophosphorylated PLB mutant, prevents HF occurrence or progression in small and large animal models [12, 14, 23]. To understand the molecular basis of the therapeutic effectiveness of S16E, we previously studied its structural dynamics, showing that the S16E mutation does not abolish SERCA binding, but it partially unfolds the cytoplasmic domain of PLB (detected by EPR and NMR) [6, 22], almost as much as is caused by phosphorylation at S16 [20, 22, 24]. We suggest that S16E can relieve SERCA inhibition by competing with PLB_W for SERCA binding.

In the present study, we test this hypothesis directly and quantitatively by performing both FRET and functional assays on reconstituted membranes containing donor-labeled SERCA, acceptor-labeled PLB_W, and unlabeled S16E. We ask whether this LOF mutant of PLB can compete with the native WT for SERCA binding, which should reduce both FRET and inhibition (Fig. 1C). We use a similar approach to evaluate the LOF PLB mutant L31A [5] as a phosphorylatable alternative to S16E. The results have important implications for future efforts in gene therapy.

2. Materials and Methods

2.1. SERCA Purification and Labeling

SERCA was purified [25] and labeled with IAEDANS [18] as described previously. To determine the dye concentration in labeled samples, the absorbance (ε_{334nm} = 6100 M-1 cm-1) [26], was taken after treatment with 0.1M NaOH and 1% SDS. Samples of AEDANS-SERCA were flash-frozen and stored in the dark at −80°C until further usage.

2.2. Synthesis, Purification, and Labeling of PLB Mutants

PLB was assembled on Fmoc-Leu-PEG-PS resin by Fmoc chemistry using a PE Biosystems Pioneer™ peptide synthesis system, as previously reported [18]. The *N*-terminal amino

group of unlabeled PLBs was acetylated using acetic anhydride. For FRET, PLB_W was labeled at the N-terminus with the non-fluorescent acceptor Dabcyl-SE (denoted Dab-PLB_W). Peptide composition and concentration were confirmed by MALDI-TOF and amino acid analysis, and samples were stored in methanol at −20°C.

2.3. Co-reconstitution of SERCA and PLB

SERCA and PLB were co-reconstituted, as previously described [27–29], at 700 lipids/SERCA and various PLB/SERCA ratios. Each sample contained 40μg of SERCA and varying amounts of PLB to obtain molar ratios of 0–20 PLB to SERCA. Ca^{2+}-ATPase activity and FRET measurements were performed immediately after co-reconstitution.

2.4. Ca^{2+}-ATPase Functional Measurements

Functional and FRET measurements were carried out at 25°C. ATPase activity was measured as a function of [Ca^{2+}] in 96-well microtiter plates [28, 30]. The time-dependence of absorbance at 340 nm was measured in a SpectraMaxPlus™ microplate reader (Molecular Devices, Sunnyvale, CA). Data were fitted using the Hill function:

$$V=V_{\max}/[1+10^{-n(\mathrm{p}K\mathrm{Ca}-\mathrm{pCa})}], \qquad \text{Equation 1}$$

where V is the initial ATPase rate and n is the Hill coefficient. The inhibitory effect of each PLB variant was indicated by the observed increase in the apparent Ca^{2+} dissociation constant K_{Ca}, measured relative to SERCA reconstituted in the absence of PLB.

Based on K_{Ca} measured as above, we define inhibitory potency, P, as the % increase in K_{Ca} (decrease in apparent Ca^{2+} affinity) caused by PLB:

$$P(n)=[K_{Ca}(n)/K_{Ca}(0)-1]^{*}100\%, \qquad \text{Equation 2}$$

where n = PLB/SERCA.

To determine the apparent affinity of each PLB variant for SERCA, $P(n)$ data in Fig. 2*B* were fitted using the specific binding function:

$$P(n)=P_{\max}{}^{*}n/(n+K_{\mathrm{d}}), \qquad \text{Equation 3}$$

where K_d is the apparent dissociation constant.

We assume that the effects of a mixture of PLB_W with a LOF PLB_M (Fig. 3) on the SERCA K_{Ca} depends on the relative potencies and affinities of the PLB variants competing for a single inhibitory binding site on SERCA:

$$P(w+m)=\{[w^{*}P(w)+A^{*}m^{*}P(m)]/(w+\mathrm{A}^{*}m)\}, \qquad \text{Equation 4}$$

where w = PLB_W/SERCA; m = PLB_M/SERCA; $A = K_d(PLB_W)/K_d(PLB_M)$.

2.5. Fluorescence Resonance Energy Transfer (FRET) Measurements

Fluorescence emission spectra were acquired using a Gemini EM microplate fluorimeter (Molecular Devices, Sunnyvale, CA) with excitation at 350 nm from a Xenon flash lamp (1 Joule/flash). Samples were plated in triplicate (75 μL per well) on 384-well, black wall,

optical bottom well plates (Nalge Nunc International, Rochester, NY). Emission spectra were recorded in triplicate, from 420 nm to 600 nm, with a 2 nm step size, and a 420 nm long-pass emission filter. The fractional decrease in the integrated fluorescence emission of the donor (AEDANS-SERCA) caused by the presence of an acceptor (Dab-PLB_W) is defined as the FRET efficiency $E = 1 - (F_{D+A}/F_D)$, where F_{D+A} and F_D are the fluorescence intensities in the presence and absence of acceptor. If the acceptor-labeled PLB binds to a single specific binding site with a dissociation constant K_d, then

$$E=E_{max}^{*}[\mathrm{PLB}]/(K_d+[\mathrm{PLB}]), \quad \text{Equation 5}$$

where E_{max} is the limiting value of E for the SERCA-PLB complex at saturation, and [PLB] and K_d are in 2-dimensional units, PLB per 1000 lipids [18]. For convenience, titration curves are plotted below with units of PLB/SERCA on the abscissa, but the units are converted to PLB per 1000 lipids to calculate meaningful K_d values. In the competition experiments, when AEDANS-SERCA is co-reconstituted with Dab-PLB_W and unlabeled PLB_M, E depends on the relative affinities of the co-existing PLBs competing for binding to SERCA:

$$E(w+m)=w^{*}E(w)/(w+\mathrm{A}^{*}m), \quad \text{Equation 6}$$

where w, m, A, E are as defined as in Equation 4. Equation 6 is simpler than Equation 4 because PLB_M is unlabeled, so $E(m) = 0$.

3. Results

3.1. Effects of Synthetic PLB and its Mutants on SERCA K_{Ca}

The effects of synthetic PLB variants on K_{Ca}, the apparent Ca^{2+}-affinity of SERCA, were determined in co-reconstituted samples of well-defined lipid/SERCA, and PLB/SERCA. At the approximately physiological level of 5PLB/SERCA [31], all PLB variants decrease the apparent Ca^{2+} affinity of SERCA (K_{Ca} values in Fig. 2*A*). This pattern of potency is consistent with previous results using recombinant PLB variants [5, 6, 28, 32, 33]; I40A inhibits much more than PLB_W, while S16E and L31A inhibit much less. While I40A is predominantly monomeric, the other three PLB variants have been shown to be primarily pentameric, [5, 34, 35], so loss of inhibitory function is not due to differences in PLB oligomeric stability.

To further characterize the inhibitory potencies of these PLB mutants, we performed co-reconstitution varying PLB/SERCA from 0 to 20 (maintaining 700 lipids/SERCA), thus probing the normal physiological range (PLB/SERCA ≤ 5), as well as the pathophysiological range (PLB/SERCA > 5) that is often present in failing myocardium [36, 37]. Potency profiles are given in Fig. 2B, along with fits to Equation 3. As expected, the saturating potency, P_{max}, of I40A (345 ± 3%) is about 3 times that of PLB_W (120 ± 6%) [5, 28, 32], whereas both LOF PLB_M have P_{max} values about 3 times less than that of PLB_W (43 ± 7% for S16E, 35 ± 10% for L31A). Surprisingly, the apparent affinities of PLB_W and I40A for SERCA obtained from fitting their potency profiles in Fig. 2B are not significantly different: K_d values (PLB/1000 lipids) are 4.1 ± 0.8 (PLB_W), 4.0 ± 0.4 (I40A), 5.1 ± 1.1 (S16E), and 9.1 ± 4.9 (L31A). We conclude that the differences in potency displayed by these PLB variants reflect mainly the intrinsic potency of the SERCA-PLB complex at saturation, P_{max}, not the binding affinity, $1/K_d$ (Equation 3).

3.2. Functional Competition between PLB_W and LOF PLB_M

To determine whether LOF PLB_M can attenuate the inhibition of SERCA induced by PLB_W, we co-reconstituted SERCA with mixtures of PLB_W and each of the LOF PLB_M (S16E and L31A). In Fig. 3, triangles illustrate the measured potencies of SERCA/PLB_W/PLB_M mixtures at 1/2/2, 1/2/5, 1/5/5, and 1/5/10. Functional competition data are displayed relative to the inhibition profile of PLB_W from Fig. 2B (as upper bound, Fig. 3 dashed line) and an average of LOF PLB_M profiles from Fig. 2B (as lower bound, Fig. 3 dotted line). For each sample containing *w* PLB_W and *m* PLB_M mixtures, the increase in K_{Ca} is significantly smaller than for the corresponding reference samples containing only *w* PLB_W. This is the relevant effect for gene therapy applications. These experimental data, reflecting the functional competition of PLB_M with PLB_W for SERCA binding (Fig. 3 symbols), were fitted using Equation 4, yielding apparent K_d values (PLB_M/1000 lipid) of 3.2 ± 0.5 for S16E and 3.5 ± 0.6 for L31A. These are similar to the K_d values measured directly from the functional potency profiles of these PLB_M (Fig. 2B, Equation 3).

3.3. FRET measurement of competition between PLB_W and LOF PLB_M

We measured FRET between AEDANS-SERCA and Dab-PLB_W co-reconstituted in lipid over a range of PLB/SERCA. Lipids/SERCA was fixed at 700. The resulting FRET profile (Fig. 4, circles) allows a direct determination of PLB's binding affinity for SERCA, as previously shown [18]. The dashed line represents the best fit to Equation 5, giving K_d = 1.2 ± 0.3 PLB/1000 lipids. This affinity is significantly tighter than indicated by the functional profile (Fig. 2B, PLB_W), suggesting that some binding occurs without inhibition. To determine whether PLB_M and PLB_W physically compete for SERCA binding, we co-reconstituted AEDANS-SERCA, Dabcyl-PLB_W, and unlabeled LOF PLB_M at SERCA/PLB_W/PLB_M = 1/2/m (m= 2, 4, 8). As in the case of functional competition, FRET is decreased by both PLB_M (Fig. 4, triangles are below circles), indicating competition with PLB_W for binding to SERCA. Thus, both unlabeled LOF mutants PLB_M compete physically with labeled PLB_W (Fig. 4). This FRET competition data was fitted using Equation 6, yielding K_d values (PLB/1000 lipids) for the two PLB_M binding to SERCA that were indistinguishable: 1.8 ± 0.5 for S16E and 2.2 ± 0.8 for L31A.

4. Discussion

By varying the molar ratio of PLB/SERCA and measuring the Ca^{2+}-dependence of SERCA activity, we found that the potency profiles, *P*(n), of all four PLB variants are characterized by indistinguishable affinities ($1/K_d$) (Fig. 2A), despite saturating potencies (P_{max}) that vary by a factor of 10 (I40A≫PLB_W>S16E>L31A) (Fig. 2B). We conclude that, for these PLB variants, the inhibition in the SERCA-PLB complex at saturation (P_{max}) is essentially independent of affinity. This result suggests that the two LOF PLB_M should compete effectively with PLB_W for SERCA binding, thus relieving SERCA inhibition. The functional competition data (Fig. 3) supports this hypothesis – both S16E and L31A compete effectively with PLB_W to decrease the net potency (shift in K_{Ca}). Indeed, the K_d values of S16E and L31A calculated from the functional competition measurements (3.2 ± 0.5 for S16E and 3.5 ± 0.6 from L31A, Fig. 3) are even slightly smaller (greater affinity) than calculated from the potency profiles (5.1 ± 1.1 for S16E and 9.1 ± 4.9 for L31A Fig. 2B). The similar SERCA affinity of PLB_W and LOF PLB_M is further supported by the FRET data, which demonstrate physical competition between these PLB variants (Fig. 4).

These results (1) provide a rational explanation for the success of S16E-based gene therapy in animal models of heart failure [12, 14, 23], (2) further support the notion that decreased potency of PLB_M is distinct from binding affinity, and (3) demonstrate convenient, rapid methods for *in vitro* testing future PLB_M candidates for HF therapies. Indeed, the L31A

mutant may already be superior to S16E as a therapeutic candidate, because it can be phosphorylated by PKA at Ser 16, thus providing a level of adrenergic response that S16E lacks. Although the current collection of PLB variants does not show significant variation in K_d, the observation that P_{max} is uncoupled from K_d supports the hypothesis that more LOF PLBs can be designed that have either (a) a lower P_{max} than S16E or L31A, without decreasing affinity, or (b) a higher affinity without increasing P_{max}. Indeed, previous studies with PLB mutants show that insight into structure-function correlations, gained from EPR and NMR analysis of PLB structural dynamics and function, can be used effectively to guide the PLB_M engineering process [6, 22].

HIGHLIGHTS

- Explanation for success of S16E-based gene therapy in heart failure animal models.
- Decreased potency of PLB mutants is distinct from binding affinity.
- *In vitro* testing of future PLB mutant candidates for heart failure therapies.

Acknowledgments

We thank Gianluigi Veglia for helpful discussions, Cory I. Paterson and Zhiwen Zhang for excellent technical assistance, and Octavian Cornea for preparing the manuscript for publication.

This work was supported, in part, by a grant to D.D.T. (NIH GM27906). E.L.L. was supported by NIH Chemical Biology Training Grant (NIH GM870008), followed by a predoctoral fellowship from the American Heart Association (Midwest Affiliate 0815604G).

Abbreviations

Ca^{2+}	divalent calcium ion
Dabcyl-SE	4-((4-(dimethylamino)phenyl)azo)-benzoic acid succinimidyl ester
Fmoc	9-fluorenylmethyloxycarbonyl
FRET	fluorescence resonance energy transfer
IAEDANS	5-((((2-iodoacetyl)amino)ethyl)amino) naphthalene-1-sulfonic acid
K_d	dissociation constant
LOF	loss of function
MALDI-TOF	matrix-assisted laser desorption/ionization time-of-flight mass spectroscopy
NaOH	Sodium hydroxide
pCa	$-\log[Ca^{2+}]$
PKA	protein kinase A
PEG-PS	polyethylene glycol–polystyrene (graft support)
pK_{Ca}	$-\log(K_{Ca})$, calcium concentration at half-maximal ATPase activity
PLB	phospholamban
SDS	Sodium dodecyl-sulfate
SERCA	Sarco-endoplasmic reticulum Ca^{2+}-ATPase

SR	sarcoplasmic reticulum
WT	wild-type

References

1. Cantilina T, Sagara Y, Inesi G, Jones LR. Comparative studies of cardiac and skeletal sarcoplasmic reticulum ATPases. Effect of a phospholamban antibody on enzyme activation by Ca2+ J Biol Chem. 1993; 268:17018–17025. [PubMed: 8349590]
2. Chien KR, Ross J Jr, Hoshijima M. Calcium and heart failure: the cycle game. Nat Med. 2003; 9:508–509. [PubMed: 12724757]
3. Simmerman HK, Jones LR. Phospholamban: protein structure, mechanism of action, and role in cardiac function. Physiol Rev. 1998; 78:921–947. [PubMed: 9790566]
4. Simmerman HK, Collins JH, Theibert JL, Wegener AD, Jones LR. Sequence analysis of phospholamban. Identification of phosphorylation sites and two major structural domains. J Biol Chem. 1986; 261:13333–13341. [PubMed: 3759968]
5. Kimura Y, Kurzydlowski K, Tada M, MacLennan DH. Phospholamban inhibitory function is activated by depolymerization. J Biol Chem. 1997; 272:15061–15064. [PubMed: 9182523]
6. Ha KN, Traaseth NJ, Verardi R, Zamoon J, Cembran A, Karim CB, Thomas DD, Veglia G. Controlling the inhibition of the sarcoplasmic Ca2+-ATPase by tuning phospholamban structural dynamics. J Biol Chem. 2007; 282:37205–37214. [PubMed: 17908690]
7. Roger VL, Go AS, Lloyd-Jones DM, Adams RJ, Berry JD, Brown TM, Carnethon MR, Dai S, de Simone G, Ford ES, Fox CS, Fullerton HJ, Gillespie C, Greenlund KJ, Hailpern SM, Heit JA, Ho PM, Howard VJ, Kissela BM, Kittner SJ, Lackland DT, Lichtman JH, Lisabeth LD, Makuc DM, Marcus GM, Marelli A, Matchar DB, McDermott MM, Meigs JB, Moy CS, Mozaffarian D, Mussolino ME, Nichol G, Paynter NP, Rosamond WD, Sorlie PD, Stafford RS, Turan TN, Turner MB, Wong ND, Wylie-Rosett J. Heart disease and stroke statistics--2011 update: a report from the American Heart Association. Circulation. 123:e18–e209. [PubMed: 21160056]
8. Lipskaia L, Chemaly ER, Hadri L, Lompre AM, Hajjar RJ. Sarcoplasmic reticulum Ca(2+) ATPase as a therapeutic target for heart failure. Expert Opin Biol Ther. 2010; 10:29–41. [PubMed: 20078230]
9. MacLennan DH, Kranias EG. Phospholamban: a crucial regulator of cardiac contractility. Nature Reviews. 2003; 4:666–678.
10. Minamisawa S, Hoshijima M, Chu G, Ward CA, Frank K, Gu Y, Martone ME, Wang Y, Ross J Jr, Kranias EG, Giles WR, Chien KR. Chronic phospholamban-sarcoplasmic reticulum calcium ATPase interaction is the critical calcium cycling defect in dilated cardiomyopathy. Cell. 1999; 99:313–322. [PubMed: 10555147]
11. del Monte F, Harding SE, Dec GW, Gwathmey JK, Hajjar RJ. Targeting phospholamban by gene transfer in human heart failure. Circulation. 2002; 105:904–907. [PubMed: 11864915]
12. Iwanaga Y, Hoshijima M, Gu Y, Iwatate M, Dieterle T, Ikeda Y, Date MO, Chrast J, Matsuzaki M, Peterson KL, Chien KR, Ross J Jr. Chronic phospholamban inhibition prevents progressive cardiac dysfunction and pathological remodeling after infarction in rats. J Clin Invest. 2004; 113:727–736. [PubMed: 14991071]
13. Meyer M, Belke DD, Trost SU, Swanson E, Dieterle T, Scott B, Cary SP, Ho P, Bluhm WF, McDonough PM, Silverman GJ, Dillmann WH. A recombinant antibody increases cardiac contractility by mimicking phospholamban phosphorylation. Faseb J. 2004; 18:1312–1314. [PubMed: 15180962]
14. Hoshijima M, Ikeda Y, Iwanaga Y, Minamisawa S, Date MO, Gu Y, Iwatate M, Li M, Wang L, Wilson JM, Wang Y, Ross J Jr, Chien KR. Chronic suppression of heart-failure progression by a pseudophosphorylated mutant of phospholamban via in vivo cardiac rAAV gene delivery. Nat Med. 2002; 8:864–871. [PubMed: 12134142]
15. Haghighi K, Kolokathis F, Pater L, Lynch RA, Asahi M, Gramolini AO, Fan GC, Tsiapras D, Hahn HS, Adamopoulos S, Liggett SB, Dorn GW 2nd, MacLennan DH, Kremastinos DT, Kranias

EG. Human phospholamban null results in lethal dilated cardiomyopathy revealing a critical difference between mouse and human. J Clin Invest. 2003; 111:869–876. [PubMed: 12639993]

16. James P, Inui M, Tada M, Chiesi M, Carafoli E. Nature and site of phospholamban regulation of the Ca2+ pump of sarcoplasmic reticulum. Nature. 1989; 342:90–92. [PubMed: 2530454]
17. Chen Z, Akin BL, Jones LR. Mechanism of reversal of phospholamban inhibition of the cardiac Ca2+-ATPase by protein kinase A and by anti-phospholamban monoclonal antibody 2D12. J Biol Chem. 2007; 282:20968–20976. [PubMed: 17548345]
18. Mueller B, Karim CB, Negrashov IV, Kutchai H, Thomas DD. Direct detection of phospholamban and sarcoplasmic reticulum Ca-ATPase interaction in membranes using fluorescence resonance energy transfer. Biochemistry. 2004; 43:8754–8765. [PubMed: 15236584]
19. Li J, Bigelow DJ, Squier TC. Conformational changes within the cytosolic portion of phospholamban upon release of Ca-ATPase inhibition. Biochemistry. 2004; 43:3870–3879. [PubMed: 15049694]
20. Karim CB, Zhang Z, Howard EC, Torgersen KD, Thomas DD. Phosphorylation-dependent conformational switch in spin-labeled phospholamban bound to SERCA. J Mol Biol. 2006; 358:1032–1040. [PubMed: 16574147]
21. Chen Z, Stokes DL, Jones LR. Role of leucine 31 of phospholamban in structural and functional interactions with the Ca2+ pump of cardiac sarcoplasmic reticulum. J Biol Chem. 2005; 280:10530–10539. [PubMed: 15644311]
22. Gustavsson M, Traaseth NJ, Karim CB, Lockamy EL, Thomas DD, Veglia G. Lipid-Mediated Folding/Unfolding of Phospholamban as a Regulatory Mechanism for the Sarcoplasmic Reticulum Ca(2+)-ATPase. J Mol Biol. 2011
23. Kaye DM, Preovolos A, Marshall T, Byrne M, Hoshijima M, Hajjar R, Mariani JA, Pepe S, Chien KR, Power JM. Percutaneous cardiac recirculation-mediated gene transfer of an inhibitory phospholamban peptide reverses advanced heart failure in large animals. J Am Coll Cardiol. 2007; 50:253–260. [PubMed: 17631218]
24. Traaseth NJ, Thomas DD, Veglia G. Effects of Ser16 phosphorylation on the allosteric transitions of phospholamban/Ca(2+)-ATPase complex. J Mol Biol. 2006; 358:1041–1050. [PubMed: 16564056]
25. Stokes DL, Green NM. Three-dimensional crystals of CaATPase from sarcoplasmic reticulum. Symmetry and molecular packing. Biophys J. 1990; 57:1–14. [PubMed: 2137017]
26. Vanderkooi JM, Ierokomas A, Nakamura H, Martonosi A. Fluorescence energy transfer between Ca2+ transport ATPase molecules in artificial membranes. Biochemistry. 1977; 16:1262–1267. [PubMed: 139160]
27. Reddy LG, Autry JM, Jones LR, Thomas DD. Co-reconstitution of phospholamban mutants with the Ca-ATPase reveals dependence of inhibitory function on phospholamban structure. J Biol Chem. 1999; 274:7649–7655. [PubMed: 10075652]
28. Reddy LG, Cornea RL, Winters DL, McKenna E, Thomas DD. Defining the molecular components of calcium transport regulation in a reconstituted membrane system. Biochemistry. 2003; 42:4585–4592. [PubMed: 12693956]
29. Reddy LG, Jones LR, Pace RC, Stokes DL. Purified, reconstituted cardiac Ca2+-ATPase is regulated by phospholamban but not by direct phosphorylation with Ca2+/calmodulin- dependent protein kinase. J Biol Chem. 1996; 271:14964–14970. [PubMed: 8663079]
30. Karim CB, Paterlini MG, Reddy LG, Hunter GW, Barany G, Thomas DD. Role of cysteine residues in structural stability and function of a transmembrane helix bundle. J Biol Chem. 2001; 276:38814–38819. [PubMed: 11477077]
31. Ferrington D, Moewe P, Yao Q, Bigelow D. Comparison of the stoichiomtery of phospholamban to SERCA2a in cardiac and skeletal muscle. Biophys J. 1998; 74:356–361.
32. Cornea RL, Autry JM, Chen Z, Jones LR. Reexamination of the role of the leucine/isoleucine zipper residues of phospholamban in inhibition of the Ca2+ pump of cardiac sarcoplasmic reticulum. J Biol Chem. 2000; 275:41487–41494. [PubMed: 11016944]
33. Zvaritch E, Backx PH, Jirik F, Kimura Y, de Leon S, Schmidt AG, Hoit BD, Lester JW, Kranias EG, MacLennan DH. The transgenic expression of highly inhibitory monomeric forms of

phospholamban in mouse heart impairs cardiac contractility. J Biol Chem. 2000; 275:14985–14991. [PubMed: 10809743]

34. Toyofuku T, Kurzydlowski K, Tada M, MacLennan DH. Amino acids Glu2 to Ile18 in the cytoplasmic domain of phospholamban are essential for functional association with the Ca(2+)-ATPase of sarcoplasmic reticulum. J Biol Chem. 1994; 269:3088–3094. [PubMed: 7905483]
35. Simmerman HKB, Kobayashi YM, Autry JM, Jones LR. A Leucine Zipper Stabilizes the Pentameric Membrane Domain of Phospholamban and Forms a Coiled-coil Pore Structure. J. Biol. Chem. 1996; 271:5941–5946. [PubMed: 8621468]
36. Meyer M, Schillinger W, Pieske B, Holubarsch C, Heilmann C, Posival H, Kuwajima G, Mikoshiba K, Just H, Hasenfuss G, et al. Alterations of sarcoplasmic reticulum proteins in failing human dilated cardiomyopathy. Circulation. 1995; 92:778–784. [PubMed: 7641356]
37. Dash R, Frank KF, Carr AN, Moravec CS, Kranias EG. Gender influences on sarcoplasmic reticulum Ca2+-handling in failing human myocardium. J Mol Cell Cardiol. 2001; 33:1345–1353. [PubMed: 11437540]

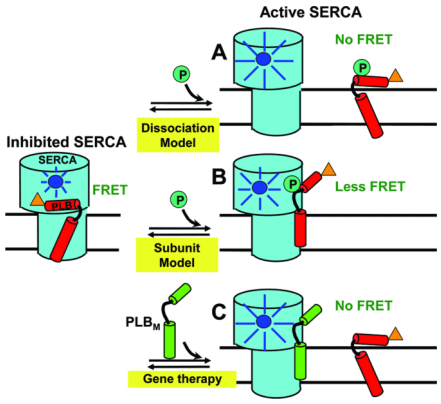

Fig. 1. Models for relief of SERCA inhibition

Left: PLB_W binding to SERCA is detected when the fluorescence of donor (blue) on SERCA is quenched by the acceptor (orange) on PLB via FRET. (A) In the Dissociation Model, loss of function (e.g., due to phosphorylation) requires dissociation of the SERCA-PLB complex, which would completely eliminate FRET. (B) In the Subunit Model, inhibition can be relieved by a structural rearrangement, without dissociation of the SERCA-PLB complex. (C) For HF gene therapy applications, if a LOF mutant PLB_M has affinity for SERCA comparable to that of PLB_W, it can compete with PLB_W to increase SERCA function. These hypotheses can be tested by FRET.

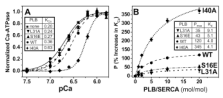

Fig. 2. Effect of PLB mutants on the apparent Ca^{2+}-affinity of SERCA

(A) Ca^{2+} dependence of ATPase activity of SERCA reconstituted in lipid in the absence of PLB or in the presence of 5 moles of PLB per mole of SERCA. Activity is normalized relative to V_{max}, along with fits using the Hill function (Equation 1), with best-fit K_{Ca} (μM) values in inset table. (B) Dependence of PLB inhibitory potency (P, Equation 2) on PLB/SERCA, along with fits to the data using Equation 3, with best-fit P_{max} (%) and K_d (PLB/1000 lipids) values in inset table. Each plotted symbol represents mean ± SEM from at least three measurements.

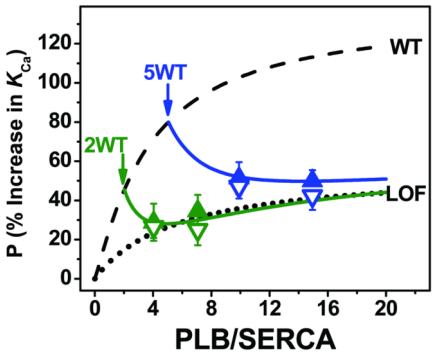

Fig. 3. Functional competition

Effects of LOF PLB_M (S16E solid triangles, L31A open triangles) on inhibitory potency in the presence of 2 (green) and 5 (blue) PLB_W/SERCA. Dashed curve: PLB_W alone (Fig. 2B). Dotted curve: averaged PLB_M profile (Fig. 2B). Solid curves represent fits to the competition data using Equation 4. Each plotted point is the mean ± SEM from at least three measurements.

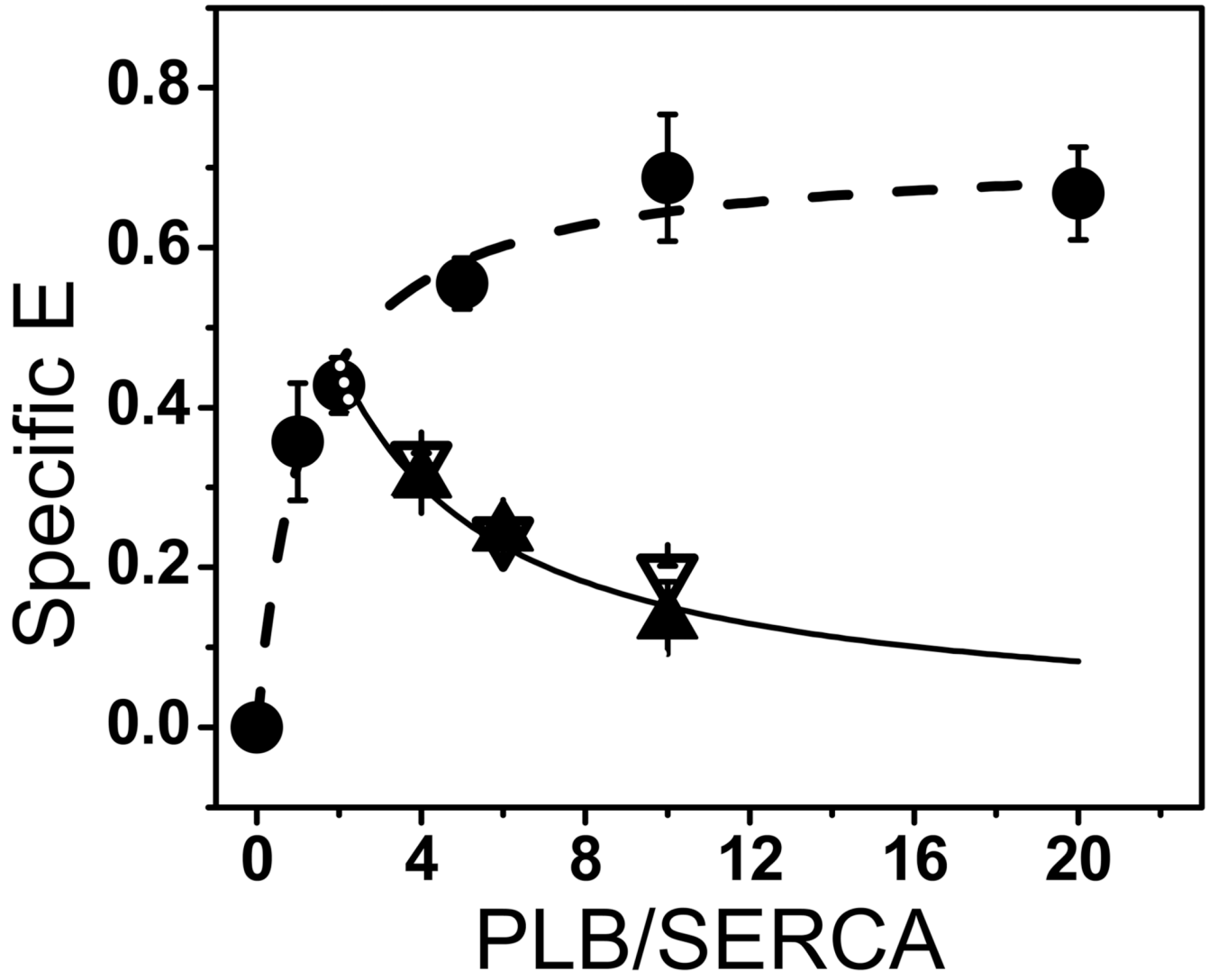

Fig. 4. FRET Competition

The dependence of FRET $E(w)$ on the ratio w of Dab-PLB_W to AEDANS-SERCA (circles) was fitted using Equation 3 (dashed curve), giving K_d = 1.2 ± 0.3 PLB/1000 lipids. FRET competition data, $E(w+m)$, are shown for w = 2 Dab-PLB_W and m = 2, 4, or 8 unlabeled PLB_M (S16E closed triangles, L31A open triangles). Solid curve shows the best fit of the averaged PLB_M data to Equation 6, giving K_d = 2.0 ± 0.9 PLB/1000 lipids. Each plotted point represents the mean ± SEM from at least three measurements.